The Optical Gravitational Lensing Experiment. Cepheids in the Magellanic Clouds. VI. Double-Mode Cepheids in the Large Magellanic Cloud*

I. Soszyński[1], A. Udalski[1], M. Szymański[1], M. Kubiak[1], G. Pietrzyński[1,2], P. Woźniak[3], and K. Żebruń[1]

[1]Warsaw University Observatory, Al. Ujazdowskie 4, 00-478 Warszawa, Poland
e-mail: (soszynsk,udalski,msz,mk,pietrzyn,zebrun)@astrouw.edu.pl
[2] Universidad de Concepción, Departamento de Fisica, Casilla 160–C, Concepción, Chile
[3] Princeton University Observatory, Princeton, NJ 08544-1001, USA
e-mail: wozniak@astro.princeton.edu

ABSTRACT

We present a sample of 76 double-mode Cepheids detected in the 4.5 square degree area in the central part of the LMC. 19 stars from the sample pulsate in the fundamental mode and the first overtone while 57 objects are the first and second overtone pulsators.

We analyze the period ratio of double-mode Cepheids and Fourier parameters of decomposition of the light curves of these objects. We also present location of different type Cepheids from the LMC in the color-magnitude diagram and show the distribution of their $V-I$ color indices.

1 Introduction

Observations of double-mode Cepheids provide many information about evolution and structure of massive stars. Parameters of these stars that can be measured with high precision, like periods, period ratios and Fourier coefficients of light curve decomposition, can give us important information not only on the basic physical parameters of these stars but also on chemical composition or distance to them.

Only 14 double-mode Cepheids are known in the Galaxy (Pardo and Poretti 1997). In this sample only one object, CO Aur, pulsates simultaneously in the first and the second overtone (FO/SO) modes. The remaining Galactic double-mode Cepheids have the fundamental mode and the first overtone excited (FU/FO). Cepheids pulsating in two radial modes are difficult to discover, because of the large number of datapoints required to detect and characterize

*Based on observations obtained with the 1.3 m Warsaw telescope at the Las Campanas Observatory of the Carnegie Institution of Washington.

them. Gravitational microlensing surveys provide unique observational material for search for double mode Cepheids. Regular, long term photometric observations of high stellar density regions of the sky, are ideal for examining variable stars, including double-mode Cepheids.

Forty five double-mode Cepheids were identified in the Large Magellanic Clouds by the MACHO microlensing team (Alcock *et al.* 1995). This sample, increased later to 75 objects (Alcock *et al.* 1999), allowed detailed study of properties of these objects. Based on the Fourier decomposition of FO/SO double-mode Cepheids light curves, Alcock *et al.* (1999) characterized properties of the second overtone pulsations, what led to detection of potential candidates for the single-mode second overtone Cepheids (Alcock *et al.* 1999, Udalski *et al.* 1999b).

The second phase of the Optical Gravitational Lensing Experiment (OGLE-II) microlensing survey started in January 1997. Since then the Large and Small Magellanic Clouds have been observed regularly, practically on every clear night. Observations were made through the BVI filters, very closely reproducing the standard BVI system. More than three years of monitoring allowed to detect and characterize thousands of Cepheids in both Magellanic Clouds including large sample of double-mode Cepheids.

In the previous papers of this series we presented analysis of 93 double-mode Cepheids detected by the OGLE team in the SMC (Udalski *et al.* 1999a), discovery of 13 candidates for Cepheids pulsating solely in the second overtone (Udalski *et al.* 1999b), analysis of the Period-Luminosity and Period-Luminosity-Color relations of Cepheids from the LMC and SMC (Udalski *et al.* 1999c) and Catalogs of Cepheids in the LMC (Udalski *et al.* 1999d) and SMC (Udalski *et al.* 1999e).

This paper, the final of this series, completes the sample of Cepheids detected in Magellanic Clouds during the second phase of the OGLE project. We present here 76 double-mode Cepheids detected in the LMC. Nineteen of these objects are stars pulsating in the fundamental mode and the first overtone, 57 are the first and the second overtone pulsators. Forty two double-mode Cepheids from our sample were previously detected by the MACHO team (Alcock *et al.* 1995, 1999), the remaining stars are detected for the first time. We provide all basic observational parameters of detected stars. Their photometry is available from the OGLE Internet archive.

2 Observations

All observations presented in this paper were carried out during the second phase of the OGLE experiment with the 1.3-m Warsaw telescope at the Las Campanas Observatory, Chile, which is operated by the Carnegie Institution of Washington. The telescope was equipped with the "first generation" camera with a SITe 2048×2048 CCD detector working in the drift-scan mode. The pixel size was 24 μm giving the 0.417 arcsec/pixel scale. Observations of the LMC were performed in the "slow" reading mode of the CCD detector with the gain

3.8 e$^-$/ADU and readout noise about 5.4 e$^-$. Details of the instrumentation setup can be found in Udalski, Kubiak and Szymański (1997).

Observations of the LMC started on January 6, 1997. 11 driftscan fields, each covering 14.2×57 arcmins on the sky, were observed during the first months of 1997. Additional 10 fields were added in October 1997 increasing the total observed area of the LMC to about 4.5 square degree. In this paper we present data collected up to the end of May 2000. Observations were obtained in the standard *BVI*-bands with the majority of measurements made in the *I*-band. The reader is referred to Udalski *et al.* (2000) for more details about methods of data reduction, tests on quality of photometric data, astrometry, location of observed fields etc.

3 Selection of Double-Mode Cepheids

The search for Cepheids in the 21 OGLE LMC fields is described in detail in Udalski *et al.* (1999d). The variable stars classified as Cepheids (about 1500 objects in total) were then searched for double-mode objects.

The selection of double-mode Cepheids was performed using identical two stage algorithm as applied for the SMC double-mode Cepheid search (Udalski *et al.* 1999a). In the first stage the observations of each Cepheid candidate were folded with the detected period, the light curve was fitted by high order polynomial and subtracted. The residuals were then searched for additional periodic signal and, if detected, such a candidate was selected for further analysis. Then a histogram of the ratio of the shorter to the longer period of double-mode Cepheid candidates was constructed. It exhibited two clear sharp peaks corresponding to the ratio of the first overtone to the fundamental period, ≈ 0.72, and the second to the first overtone period, ≈ 0.805, in good agreement with Alcock *et al.* (1995, 1999). The list of the double-mode Cepheid candidates from this search included stars having the period ratio within ± 0.02 from these values.

The second, final search for double-mode Cepheids was performed using the CLEAN algorithm of period determination (Roberts, Lehár and Dreher 1987). All 1500 objects from the LMC Cepheid candidate list were analyzed with the CLEAN period search algorithm. Having well established limits for the period ratio of double-mode Cepheids from the preliminary analysis, only those objects which exhibited suitable period ratio (± 0.015) between the highest peak in the power spectrum and one of the next four strongest peaks were further analyzed. The final list of the double-mode Cepheid candidates presented in this paper was obtained after careful visual inspection of the CLEAN power spectra of each object.

Table 1

FU/FO Double-Mode Cepheids in the LMC

Field	Star No.	RA(J2000)	DEC(J2000)	$P_{\rm FO}$ [days]	$R_{21}^{\rm FO}$	$\phi_{21}^{\rm FO}$	$P_{\rm FU}$ [days]	$R_{21}^{\rm FU}$	$\phi_{21}^{\rm FU}$	$P_{\rm FO}/P_{\rm FU}$	I [mag]	$B-V$ [mag]	$V-I$ [mag]	Remarks
LMC_SC1	158021	$5^h33^m39^s.53$	$-69^\circ54'54''.8$	2.10084	0.159	4.920	2.93701	0.228	4.462	0.71530	15.373	0.495	0.705	M
LMC_SC2	143088	$5^h31^m09^s.00$	$-70^\circ05'14''.9$	2.45578	0.106	5.127	3.44679	0.209	4.401	0.71248	15.036	0.456	0.660	M
LMC_SC2	172961	$5^h31^m00^s.05$	$-69^\circ49'16''.3$	2.64048	0.102	5.126	3.68579	0.214	4.570	0.71639	15.002	0.514	0.731	M
LMC_SC3	88012	$5^h28^m00^s.16$	$-69^\circ37'20''.5$	1.12078	0.199	4.280	1.54689	0.180	4.476	0.72454	16.304	0.452	0.652	M
LMC_SC3	415237	$5^h29^m36^s.16$	$-69^\circ40'26''.8$	2.43755	0.091	5.254	3.40504	0.158	4.570	0.71587	15.226	0.550	0.749	M
LMC_SC4	436072	$5^h27^m15^s.98$	$-69^\circ43'43''.8$	2.44086	0.085	4.930	3.43369	0.250	4.499	0.71086	15.023	0.466	0.668	M
LMC_SC6	6	$5^h20^m07^s.15$	$-70^\circ04'09''.1$	3.45325	0.103	3.704	4.84127	0.165	4.591	0.71329	14.575	0.518	0.664	M
LMC_SC6	322363	$5^h21^m54^s.69$	$-69^\circ23'05''.5$	2.34750	0.120	5.302	3.32153	0.186	4.475	0.70675	15.052	0.595	0.630	M
LMC_SC8	46345	$5^h15^m31^s.20$	$-69^\circ18'04''.4$	2.27345	0.145	5.435	3.17096	0.062	4.399	0.71696	15.367	0.604	0.724	M
LMC_SC10	278863	$5^h12^m00^s.05$	$-68^\circ48'43''.4$	0.97183	0.183	3.830	1.33356	0.000	–	0.72875	16.557	0.456	0.754	
LMC_SC13	156166	$5^h06^m29^s.53$	$-68^\circ54'20''.2$	2.73218	0.059	5.043	3.83507	0.168	4.363	0.71242	14.877	0.575	0.636	M
LMC_SC14	134553	$5^h03^m58^s.32$	$-69^\circ25'38''.3$	2.79677	0.049	5.749	3.89293	0.138	4.436	0.71842	14.896	0.430	0.708	M
LMC_SC14	220934	$5^h04^m29^s.01$	$-69^\circ09'26''.8$	0.86917	0.184	4.090	1.18466	0.285	4.118	0.73369	16.406	0.361	0.543	
LMC_SC15	69667	$5^h00^m55^s.12$	$-69^\circ16'31''.3$	1.37695	0.205	4.540	1.90412	0.171	4.378	0.72314	16.052	0.564	0.691	M
LMC_SC16	115243	$5^h35^m56^s.77$	$-70^\circ04'51''.2$	2.46751	0.065	5.147	3.45510	0.193	4.441	0.71416	15.359	0.748	0.846	M
LMC_SC16	177941	$5^h36^m54^s.86$	$-70^\circ08'10''.4$	1.29934	0.080	4.464	1.78612	0.235	4.238	0.72747	16.146	0.584	0.748	M
LMC_SC16	230285	$5^h37^m38^s.85$	$-70^\circ14'15''.9$	2.55468	0.000	–	3.56455	0.142	5.164	0.71669	15.177	0.714	0.719	S
LMC_SC17	33290	$5^h37^m38^s.84$	$-70^\circ14'15''.9$	2.55469	0.034	3.970	3.56418	0.000	–	0.71677	15.174	0.706	0.711	
LMC_SC17	191865	$5^h39^m29^s.28$	$-70^\circ38'19''.4$	0.93760	0.209	3.962	1.28511	0.201	4.739	0.72959	16.436	0.933	0.642	M
LMC_SC18	89202	$5^h41^m17^s.55$	$-70^\circ16'38''.7$	1.07321	0.265	4.501	1.47140	0.263	4.161	0.72938	16.239	0.669	0.704	M

Remarks: M: Double-mode Cepheid reported by MACHO (Alcock *et al.* 1995); S: same star as LMC_SC17 33290

T a b l e 2

FO/SO Double-Mode Cepheids in the LMC

Field	Star No.	RA(J2000)	DEC(J2000)	$P_{\rm SO}$ [days]	$R_{21}^{\rm SO}$	$\phi_{21}^{\rm SO}$	$P_{\rm FO}$ [days]	$R_{21}^{\rm FO}$	$\phi_{21}^{\rm FO}$	$P_{\rm SO}/P_{\rm FO}$	I [mag]	$B-V$ [mag]	$V-I$ [mag]	Remarks
LMC_SC1	44845	$5^{\rm h}32^{\rm m}50\overset{\rm s}{.}01$	$-70°04'15\overset{''}{.}1$	0.76599	0.079	5.072	0.95199	0.227	4.202	0.80462	16.357	0.437	0.547	
LMC_SC1	158635	$5^{\rm h}33^{\rm m}13\overset{\rm s}{.}54$	$-69°52'16\overset{''}{.}5$	0.50726	0.106	2.885	0.62897	0.238	3.438	0.80649	17.157	0.504	0.654	
LMC_SC1	285275	$5^{\rm h}34^{\rm m}34\overset{\rm s}{.}80$	$-70°18'20\overset{''}{.}1$	0.68924	0.099	4.596	0.85663	0.216	4.028	0.80459	16.515	0.467	0.608	M
LMC_SC1	285318	$5^{\rm h}35^{\rm m}11\overset{\rm s}{.}41$	$-70°17'06\overset{''}{.}4$	0.56838	0.129	4.194	0.70479	0.224	3.377	0.80645	16.827	–	–	M,S1
LMC_SC1	335559	$5^{\rm h}34^{\rm m}32\overset{\rm s}{.}02$	$-69°45'14\overset{''}{.}6$	0.60364	0.103	4.519	0.74980	0.251	3.778	0.80507	16.727	0.371	0.645	M
LMC_SC2	55596	$5^{\rm h}30^{\rm m}11\overset{\rm s}{.}97$	$-69°52'02\overset{''}{.}5$	0.75139	0.000	–	0.93255	0.192	4.098	0.80574	16.419	0.440	0.626	M
LMC_SC2	289572	$5^{\rm h}31^{\rm m}30\overset{\rm s}{.}89$	$-69°44'27\overset{''}{.}7$	0.95258	0.000	–	1.18650	0.211	4.481	0.80285	16.282	0.426	0.743	
LMC_SC3	53702	$5^{\rm h}27^{\rm m}27\overset{\rm s}{.}70$	$-69°48'07\overset{''}{.}9$	0.51014	0.145	2.858	0.63296	0.209	3.295	0.80596	16.812	0.503	0.629	S2
LMC_SC3	187331	$5^{\rm h}28^{\rm m}24\overset{\rm s}{.}13$	$-69°41'55\overset{''}{.}1$	0.41865	0.101	3.916	0.52051	0.177	2.949	0.80431	17.337	0.538	0.613	
LMC_SC3	360128	$5^{\rm h}29^{\rm m}35\overset{\rm s}{.}71$	$-70°02'57\overset{''}{.}1$	0.43604	0.280	1.653	0.54128	0.170	3.015	0.80557	16.980	0.370	0.549	
LMC_SC4	53796	$5^{\rm h}25^{\rm m}26\overset{\rm s}{.}46$	$-69°49'49\overset{''}{.}8$	1.03685	0.000	–	1.29506	0.158	4.294	0.80062	16.650	0.646	0.976	
LMC_SC4	138485	$5^{\rm h}25^{\rm m}52\overset{\rm s}{.}54$	$-70°07'18\overset{''}{.}3$	0.52044	0.000	–	0.64652	0.152	3.385	0.80499	16.806	0.423	0.516	
LMC_SC4	168269	$5^{\rm h}26^{\rm m}02\overset{\rm s}{.}18$	$-69°52'10\overset{''}{.}0$	0.58844	0.000	–	0.72924	0.167	3.503	0.80692	16.793	0.410	0.675	M
LMC_SC4	176400	$5^{\rm h}25^{\rm m}59\overset{\rm s}{.}29$	$-69°49'14\overset{''}{.}2$	0.89496	0.000	–	1.10890	0.168	3.667	0.80707	16.061	0.520	0.635	M
LMC_SC4	220148	$5^{\rm h}26^{\rm m}01\overset{\rm s}{.}36$	$-69°30'41\overset{''}{.}7$	0.59513	0.081	4.942	0.74085	0.247	3.650	0.80331	16.731	0.504	0.584	M
LMC_SC4	418294	$5^{\rm h}27^{\rm m}27\overset{\rm s}{.}69$	$-69°48'07\overset{''}{.}9$	0.51014	0.000	–	0.63296	0.202	3.267	0.80596	16.807	0.473	0.632	
LMC_SC5	186053	$5^{\rm h}23^{\rm m}14\overset{\rm s}{.}01$	$-69°36'36\overset{''}{.}2$	0.63112	0.138	4.634	0.78333	0.179	3.676	0.80569	16.577	0.404	0.553	M
LMC_SC5	338334	$5^{\rm h}23^{\rm m}59\overset{\rm s}{.}19$	$-69°15'29\overset{''}{.}6$	0.67333	0.110	4.621	0.83483	0.184	3.548	0.80655	16.513	0.467	0.635	M
LMC_SC5	338399	$5^{\rm h}23^{\rm m}49\overset{\rm s}{.}56$	$-69°13'32\overset{''}{.}9$	0.46661	0.000	–	0.57951	0.121	3.550	0.80518	16.870	–	0.501	
LMC_SC6	49297	$5^{\rm h}19^{\rm m}57\overset{\rm s}{.}16$	$-69°39'14\overset{''}{.}3$	0.41327	0.317	3.467	0.51477	0.153	4.017	0.80282	16.913	–	–	S3

Remarks: M: Double-mode Cepheid reported by MACHO (Alcock *et al.* 1999); U: uncertain; S1: same star as LMC_SC16 21126
S2: same star as LMC_SC4 418294; S3: same star as LMC_SC7 380269

T a b l e 2

Continued

Field	Star No.	RA(J2000)	DEC(J2000)	P_{SO} [days]	R_{21}^{SO}	ϕ_{21}^{SO}	P_{FO} [days]	R_{21}^{FO}	ϕ_{21}^{FO}	$P_{\mathrm{SO}}/P_{\mathrm{FO}}$	I [mag]	$B-V$ [mag]	$V-I$ [mag]	Remarks
LMC_SC6	142093	$5^{\mathrm{h}}21^{\mathrm{m}}16.^{\mathrm{s}}55$	$-69^{\circ}52'02.''6$	0.72209	0.102	4.932	0.89629	0.184	4.061	0.80564	16.462	0.417	0.572	M
LMC_SC6	260869	$5^{\mathrm{h}}21^{\mathrm{m}}25.^{\mathrm{s}}28$	$-69^{\circ}52'51.''1$	0.65260	0.117	4.697	0.80955	0.226	3.818	0.80613	16.761	0.443	0.676	M
LMC_SC6	267410	$5^{\mathrm{h}}21^{\mathrm{m}}50.^{\mathrm{s}}43$	$-69^{\circ}49'59.''4$	0.71666	0.235	5.142	0.88861	0.149	3.577	0.80650	16.586	0.572	0.644	U
LMC_SC6	413716	$5^{\mathrm{h}}22^{\mathrm{m}}10.^{\mathrm{s}}24$	$-69^{\circ}34'18.''1$	0.47452	0.000	–	0.59010	0.173	3.343	0.80413	17.040	0.385	0.568	
LMC_SC7	120511	$5^{\mathrm{h}}18^{\mathrm{m}}10.^{\mathrm{s}}15$	$-69^{\circ}50'55.''8$	1.00455	0.000	–	1.25127	0.189	4.090	0.80282	15.947	0.494	0.590	
LMC_SC7	207275	$5^{\mathrm{h}}18^{\mathrm{m}}42.^{\mathrm{s}}46$	$-69^{\circ}11'15.''2$	0.50097	0.088	4.970	0.62125	0.199	3.175	0.80639	16.925	0.506	0.579	
LMC_SC7	221814	$5^{\mathrm{h}}18^{\mathrm{m}}28.^{\mathrm{s}}01$	$-69^{\circ}03'25.''7$	0.32917	0.000	–	0.40999	0.101	2.906	0.80287	17.564	0.433	0.517	
LMC_SC7	380269	$5^{\mathrm{h}}19^{\mathrm{m}}57.^{\mathrm{s}}15$	$-69^{\circ}39'14.''4$	0.41338	0.107	0.175	0.51477	0.140	3.410	0.80304	16.845	0.322	0.518	
LMC_SC7	425296	$5^{\mathrm{h}}20^{\mathrm{m}}02.^{\mathrm{s}}63$	$-69^{\circ}23'54.''3$	0.32400	0.000	–	0.40354	0.172	2.676	0.80289	17.607	0.506	0.525	U
LMC_SC8	142	$5^{\mathrm{h}}15^{\mathrm{m}}35.^{\mathrm{s}}86$	$-69^{\circ}45'48.''3$	0.75174	0.078	4.792	0.93471	0.250	4.061	0.80425	16.403	0.664	0.540	
LMC_SC8	10158	$5^{\mathrm{h}}15^{\mathrm{m}}06.^{\mathrm{s}}51$	$-69^{\circ}39'52.''9$	0.55567	0.094	4.761	0.69000	0.235	3.406	0.80532	16.421	0.706	0.684	M,S4
LMC_SC8	81678	$5^{\mathrm{h}}15^{\mathrm{m}}35.^{\mathrm{s}}57$	$-68^{\circ}57'07.''4$	0.53637	0.110	4.088	0.66520	0.214	3.166	0.80633	16.918	0.662	0.591	M
LMC_SC8	198932	$5^{\mathrm{h}}16^{\mathrm{m}}28.^{\mathrm{s}}69$	$-69^{\circ}36'33.''1$	0.57415	0.141	4.672	0.71155	0.199	3.310	0.80690	16.819	0.509	0.582	M
LMC_SC8	218854	$5^{\mathrm{h}}16^{\mathrm{m}}28.^{\mathrm{s}}51$	$-69^{\circ}25'35.''7$	0.60137	0.200	4.018	0.74787	0.205	3.655	0.80411	16.859	0.671	0.685	M
LMC_SC8	242825	$5^{\mathrm{h}}16^{\mathrm{m}}55.^{\mathrm{s}}71$	$-69^{\circ}08'49.''7$	0.92936	0.090	4.392	1.15428	0.240	4.463	0.80514	16.132	0.460	0.598	
LMC_SC8	326147	$5^{\mathrm{h}}17^{\mathrm{m}}18.^{\mathrm{s}}24$	$-69^{\circ}16'38.''9$	0.82110	0.070	5.502	1.02239	0.231	4.151	0.80312	16.303	0.466	0.619	
LMC_SC8	337664	$5^{\mathrm{h}}17^{\mathrm{m}}20.^{\mathrm{s}}66$	$-69^{\circ}09'29.''1$	0.50728	0.000	–	0.62979	0.171	3.493	0.80547	16.718	0.480	0.480	
LMC_SC9	270100	$5^{\mathrm{h}}14^{\mathrm{m}}16.^{\mathrm{s}}93$	$-68^{\circ}54'13.''4$	0.40602	0.169	4.448	0.50487	0.258	3.261	0.80421	17.321	–	0.596	
LMC_SC9	286128	$5^{\mathrm{h}}15^{\mathrm{m}}06.^{\mathrm{s}}52$	$-69^{\circ}39'52.''9$	0.55567	0.286	4.988	0.69000	0.288	3.515	0.80532	16.415	0.573	0.715	M
LMC_SC10	204083	$5^{\mathrm{h}}11^{\mathrm{m}}39.^{\mathrm{s}}97$	$-68^{\circ}49'57.''6$	0.42292	0.000	–	0.52626	0.163	3.416	0.80363	17.202	–	–	M

Remarks: M: Double-mode Cepheid reported by MACHO (Alcock *et al.* 1999); U: uncertain; S4: same star as LMC_SC9 286128

T a b l e 2

Continued

Field	Star No.	RA(J2000)	DEC(J2000)	$P_{\rm SO}$ [days]	$R_{21}^{\rm SO}$	$\phi_{21}^{\rm SO}$	$P_{\rm FO}$ [days]	$R_{21}^{\rm FO}$	$\phi_{21}^{\rm FO}$	$P_{\rm SO}/P_{\rm FO}$	I [mag]	$B-V$ [mag]	$V-I$ [mag]	Remarks
LMC_SC11	38029	$5^{h}07^{m}36.^{s}83$	$-69^{\circ}12'46.''1$	0.97544	0.000	–	1.21809	0.191	4.185	0.80079	16.182	0.533	0.672	M
LMC_SC11	130342	$5^{h}08^{m}21.^{s}30$	$-69^{\circ}07'17.''5$	0.53341	0.218	4.108	0.66087	0.198	3.498	0.80713	16.979	0.487	0.578	
LMC_SC11	186270	$5^{h}09^{m}07.^{s}10$	$-69^{\circ}29'21.''4$	0.38792	0.000	–	0.48332	0.234	3.124	0.80262	17.523	0.514	0.640	
LMC_SC11	233290	$5^{h}09^{m}08.^{s}12$	$-68^{\circ}56'42.''9$	0.97835	0.095	4.702	1.21750	0.167	4.050	0.80357	16.022	0.519	0.646	M
LMC_SC15	16385	$5^{h}00^{m}24.^{s}15$	$-69^{\circ}14'57.''1$	0.79571	0.078	0.845	0.99044	0.253	4.164	0.80339	16.265	0.392	0.544	
LMC_SC15	85604	$5^{h}00^{m}54.^{s}79$	$-69^{\circ}03'42.''0$	0.51857	0.000	–	0.64280	0.131	3.464	0.80674	16.953	0.324	0.608	
LMC_SC15	96008	$5^{h}00^{m}38.^{s}77$	$-68^{\circ}53'55.''5$	0.79736	0.117	1.998	0.99170	0.243	4.002	0.80403	16.381	0.473	0.596	
LMC_SC15	152481	$5^{h}01^{m}48.^{s}72$	$-68^{\circ}50'44.''6$	0.89088	0.000	–	1.11021	0.269	4.147	0.80244	16.041	0.479	0.572	U
LMC_SC15	208026	$5^{h}02^{m}09.^{s}94$	$-68^{\circ}51'31.''1$	1.05956	0.064	3.742	1.32122	0.210	3.831	0.80196	15.755	0.566	0.693	M
LMC_SC16	21126	$5^{h}35^{m}11.^{s}41$	$-70^{\circ}17'06.''6$	0.56842	0.255	3.651	0.70478	0.190	3.378	0.80652	16.818	0.521	0.628	M
LMC_SC16	31616	$5^{h}35^{m}27.^{s}74$	$-70^{\circ}12'13.''4$	0.63788	0.132	4.873	0.79140	0.211	3.811	0.80601	16.907	0.562	0.717	
LMC_SC16	37231	$5^{h}35^{m}33.^{s}45$	$-70^{\circ}08'41.''5$	0.59719	0.000	–	0.74026	0.208	3.383	0.80673	16.766	0.521	0.631	
LMC_SC16	266808	$5^{h}37^{m}36.^{s}40$	$-69^{\circ}44'20.''4$	1.08041	0.178	3.603	1.35292	0.151	4.464	0.79858	16.571	0.994	1.094	M
LMC_SC17	80292	$5^{h}38^{m}45.^{s}56$	$-70^{\circ}36'11.''5$	0.65024	0.000	–	0.80782	0.228	3.657	0.80493	16.518	0.436	0.607	M
LMC_SC17	186042	$5^{h}38^{m}51.^{s}24$	$-69^{\circ}49'21.''8$	0.49119	0.140	2.244	0.61099	0.206	3.513	0.80392	17.084	–	0.669	M
LMC_SC18	199230	$5^{h}42^{m}13.^{s}76$	$-70^{\circ}09'13.''5$	0.59250	0.000	–	0.73438	0.210	3.509	0.80680	17.068	0.627	0.860	
LMC_SC20	21200	$5^{h}45^{m}22.^{s}28$	$-70^{\circ}50'11.''1$	0.89659	0.141	4.917	1.11954	0.227	4.170	0.80086	16.346	0.618	0.717	M
LMC_SC20	138333	$5^{h}46^{m}43.^{s}89$	$-70^{\circ}40'51.''4$	0.69215	0.000	–	0.85985	0.241	4.193	0.80497	16.588	0.377	0.623	M
LMC_SC20	188572	$5^{h}47^{m}12.^{s}66$	$-70^{\circ}41'13.''1$	0.81482	0.000	–	1.01544	0.212	4.007	0.80243	16.350	0.622	0.714	M
LMC_SC21	12012	$5^{h}20^{m}19.^{s}62$	$-70^{\circ}42'29.''0$	1.07489	0.087	5.251	1.34153	0.189	4.197	0.80124	15.833	0.557	0.607	M
LMC_SC21	178950	$5^{h}22^{m}06.^{s}50$	$-70^{\circ}16'11.''6$	0.86768	0.113	5.490	1.08130	0.220	4.289	0.80244	16.193	0.483	0.578	

Remarks: M: Double-mode Cepheid reported by MACHO (Alcock *et al.* 1999); U: uncertain

4 Double-Mode Cepheids in the LMC

Tables 1 and 2 list all double-mode Cepheids detected in the central area of the LMC. They contain 81 entries but only 76 objects. Five stars are located in the overlapping regions between fields and they were discovered independently in each field. Fundamental and first overtone mode pulsators (FU/FO) are listed in Table 1 while Table 2 includes objects pulsating in the first and second overtones (FO/SO). Basic parameters of each star: right ascension and declination (J2000), the intensity-mean I-band magnitude, $(B-V)$ and $(V-I)$ colors, both periods and their ratio are provided. Accuracy of periods is about $4\cdot10^{-5}P$. Finding charts for all objects are presented in Appendix A. The size of the I-band subframes is 60×60 arcsec; North is up and East to the left.

Appendices B and C show the light curves of FU/FO and FO/SO pulsators, respectively. The first and second columns in each Appendix contain original photometric data folded with the shorter and longer periods while the remaining columns show variability attributed to each mode after subtraction of the other period variability approximated by Fourier series of fifth order. For objects revealing also periodicity equal to the sum and/or difference of both mode frequencies and having an amplitude larger than twice the formal error – such terms were also subtracted from the original data. BVI photometry of all objects is available from the OGLE Internet archive (see Section 6).

Completeness of the sample is determined by completeness of the variable star search in the OGLE databases and efficiency of double-mode Cepheid detection algorithm. OGLE Cepheid catalog of the LMC was estimated to be complete in more than 96% (Udalski *et al.* 1999d). Completeness of the detection algorithm can be assessed by comparison of results obtained in the preliminary and final (CLEAN) searches. More than 90% objects in both lists are common suggesting good completeness of the search.

As a test of completeness we cross-identified double mode Cepheids reported by MACHO (Alcock *et al.* 1995, 1999). 39 out of 42 objects which are located in the OGLE fields were detected during our search. Two of the remaining objects have been misclassified, and have not entered to the list of Cepheids. One star – LMC_SC4 168269 – has a faint, close companion, and the noise in the power spectrum was greater than the peak of its second pulsation mode. All double-mode Cepheids found by the MACHO team are marked by the letter 'M' in the last column of Tables 1 and 2.

5 Discussion

Seventy six double-mode Cepheids were identified during the presented search in the 4.5 square degree area in the central part of the LMC. Nineteen objects pulsate simultaneously in the fundamental mode and first overtone while 57 objects in the first and second overtones. In the following Subsections we present the basic observational properties of detected sample.

5.1 Period Ratio in Double-Mode Cepheids

The ratio of the two periods of double-mode Cepheids is expected to be dependent on metallicity. This dependence is clearly seen in Fig. 1, which presents the period ratio of the FU/FO pulsators plotted as a function of the fundamental mode period. Beside of the LMC double-mode Cepheids we present there the period ratios of FU/FO Cepheids from the SMC (Udalski *et al.* 1999a) and the Galactic FU/FO Cepheids (Pardo and Poretti 1997). The metal contents of Cepheids in the Galaxy, LMC and SMC are approximately $Z = 0.02$, 0.008 and 0.004, respectively. It can be seen, that the lower metallicity – the higher the FU/FO period ratio of double-mode Cepheids. The best linear fit for the LMC FU/FO pulsators is given by the equation:

$$P_{\rm FO}/P_{\rm FU} = \underset{0.002}{0.734} \;-\; \underset{0.004}{0.035} \times \log P_{\rm FU}, \tag{1}$$

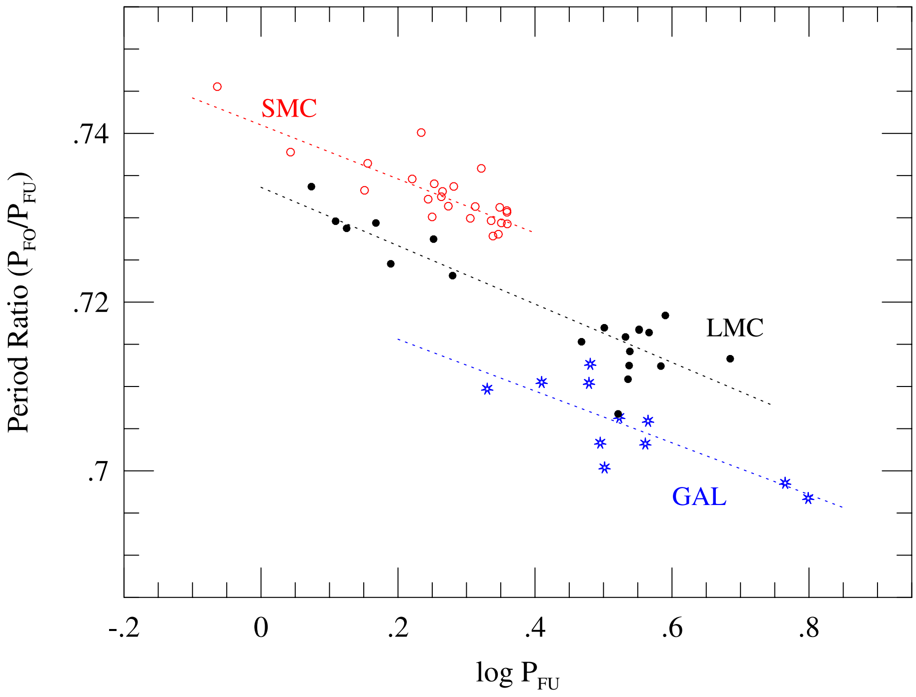

Fig. 1. Ratio of periods in FU/FO double mode Cepheids in the Galaxy and Magellanic Clouds. Dotted lines indicate the best linear fits to the observed ratios.

Period ratios for FO/SO Cepheids in LMC are almost identical with the ratios of the SMC objects. Fig. 2 presents these values in similar fashion as Fig. 1. The only one known FO/SO Galactic Cepheid (CO Aur) is also marked on the diagram. Our sample of the LMC double-mode Cepheids is numerous enough to note that the period ratio-period relation for FO/SO Cepheids is non-linear. The best square fit is as follows:

$$P_{\mathrm{SO}}/P_{\mathrm{FO}} = 0.804 - 0.020 \times \log P_{\mathrm{FO}} - 0.067 \times \log^2 P_{\mathrm{FO}}. \qquad (2)$$

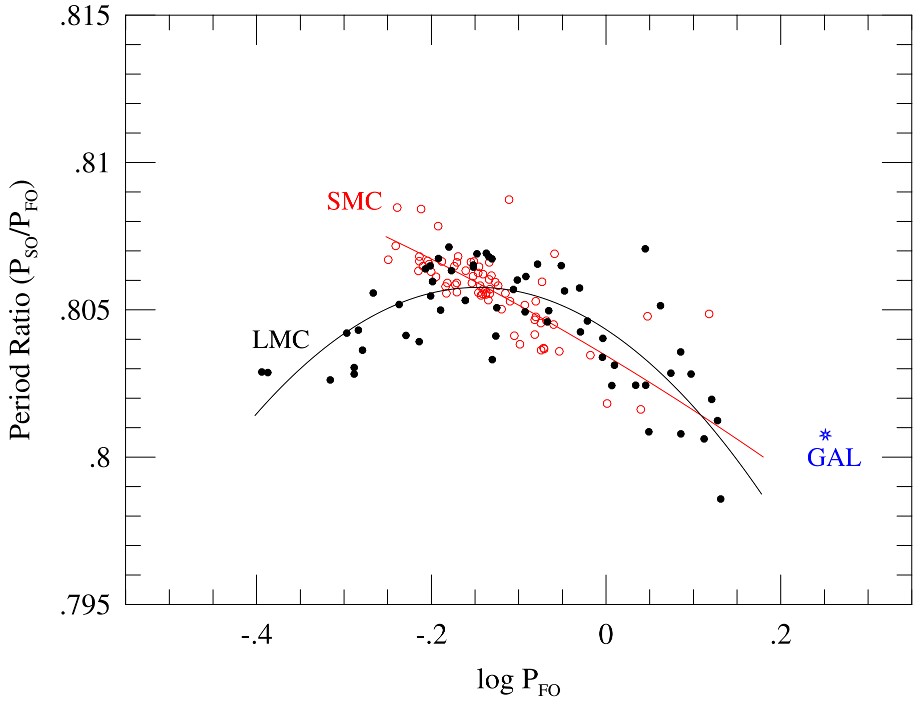

Fig. 2. Ratio of periods in FO/SO double mode Cepheids in the Galaxy and Magellanic Clouds. Thick solid line indicates the best square fit to the LMC data (filled dots) while thin line to the SMC data (open dots).

5.2 Fourier Decomposition of Light Curves of Double-Mode Cepheids

Fourier decomposition of light curves of pulsating stars has been widely used for analyzing their properties (Simon and Lee 1981). In the case of Cepheids the ratio of amplitudes of the first harmonic and the fundamental period, $R_{21} = A_2/A_1$, and phase difference, $\phi_{21} = \phi_2 - 2\phi_1$ are particularly useful. Both allow to distinguish between fundamental mode and first overtone pulsators.

Fig. 3 presents the R_{21} *vs.* $\log P$ and ϕ_{21} *vs.* $\log P$ diagrams constructed for more than 1300 single-mode Cepheids (small dots) taken from the Catalog of Cepheids from the LMC (Udalski *et al.* 1999d). The R_{21} *vs.* $\log P$ diagram shows the characteristic, well separated "V-shape" sequences for Cepheids pulsating in the fundamental mode and the first overtone. In the similar diagram ϕ_{21} *vs.*

$\log P$ the sequences for both modes of pulsation are also well defined but the separation is smaller and in some ranges of periods they overlap.

We decomposed the light curves of double-mode Cepheids to the sum of two Fourier series of fifth order corresponding to both periodicities including the terms with periodicities equal to the sum and difference of mode frequencies when their amplitudes were larger than twice the formal errors. Then we calculated R_{21} and ϕ_{21} for both pulsating modes. They are listed in Tables 1 and 2.

Fig. 3 shows positions of the FU/FO Cepheids on the R_{21} *vs.* $\log P$ and ϕ_{21} *vs.* $\log P$ diagrams. The values for the fundamental mode pulsation are plotted with large filled dots while for the first overtone mode with open circles. Objects with non-significant first harmonic amplitude, A_2, (*i.e.*, with almost sinusoidal light curve) have $R_{21}=0$ and their ϕ_{21} is not defined. Similar diagrams for FO/SO double-mode Cepheids are shown in Fig. 4. Values of R_{21} and ϕ_{21} for the first overtone pulsation are plotted with large filled dots and with open circles for the second overtone pulsations.

Figs. 3 and 4 are similar to analogous diagrams plotted for the SMC double-mode Cepheids (Udalski *et al.* 1999a). In both types of double-mode Cepheids the values of R_{21} and ϕ_{21} of first overtone pulsations fall on the sequences of the single-mode first overtone Cepheids.

Fundamental mode pulsations in the FU/FO Cepheids have much smaller values of the R_{21} parameter compared to the single-mode fundamental mode pulsators. They fall practically on the sequence of the first overtone pulsators. This means that the light curves of the fundamental mode pulsations in double-mode Cepheids are more sinusoidal than in the single-mode Cepheids of that type. However, it is clearly seen that ϕ_{21} of the fundamental mode pulsations in double-mode Cepheids fall in most cases on the single-mode fundamental mode Cepheid sequence.

Second overtone pulsations in the FO/SO Cepheids are generally small amplitude, almost sinusoidal variations (small R_{21}). Their ϕ_{21} values are usually larger than the first overtone values for similar periodicities (Fig. 4). Identical conclusions on the behavior of second overtone pulsations in double-mode Ceheids were presented by Alcock *et al.* (1999).

5.3 Color-Magnitude Diagram and Colors of Double-Mode Cepheids

Fig. 5 presents the color-magnitude diagram of subfield 2 of the LMC_SC3 field corrected for the mean $E(B-V)=0.120$ reddening in this direction (Udalski *et al.* 1999d). Tiny dots correspond to the field stars. Larger dots indicate positions of the single-mode Cepheids: fundamental mode – darker dots, first overtone – lighter dots. Positions of FU/FO double-mode Cepheids are indicated by large filled circles while FO/SO objects by star symbols.

Fig. 6 shows distribution of color indices $(V-I)_0$ of single-mode FU and FO Cepheids and double-mode FU/FO and FO/SO pulsators in the LMC. $E(B-V)$ reddening values from Table 2 of Udalski *et al.* (1999d) were used to deredden

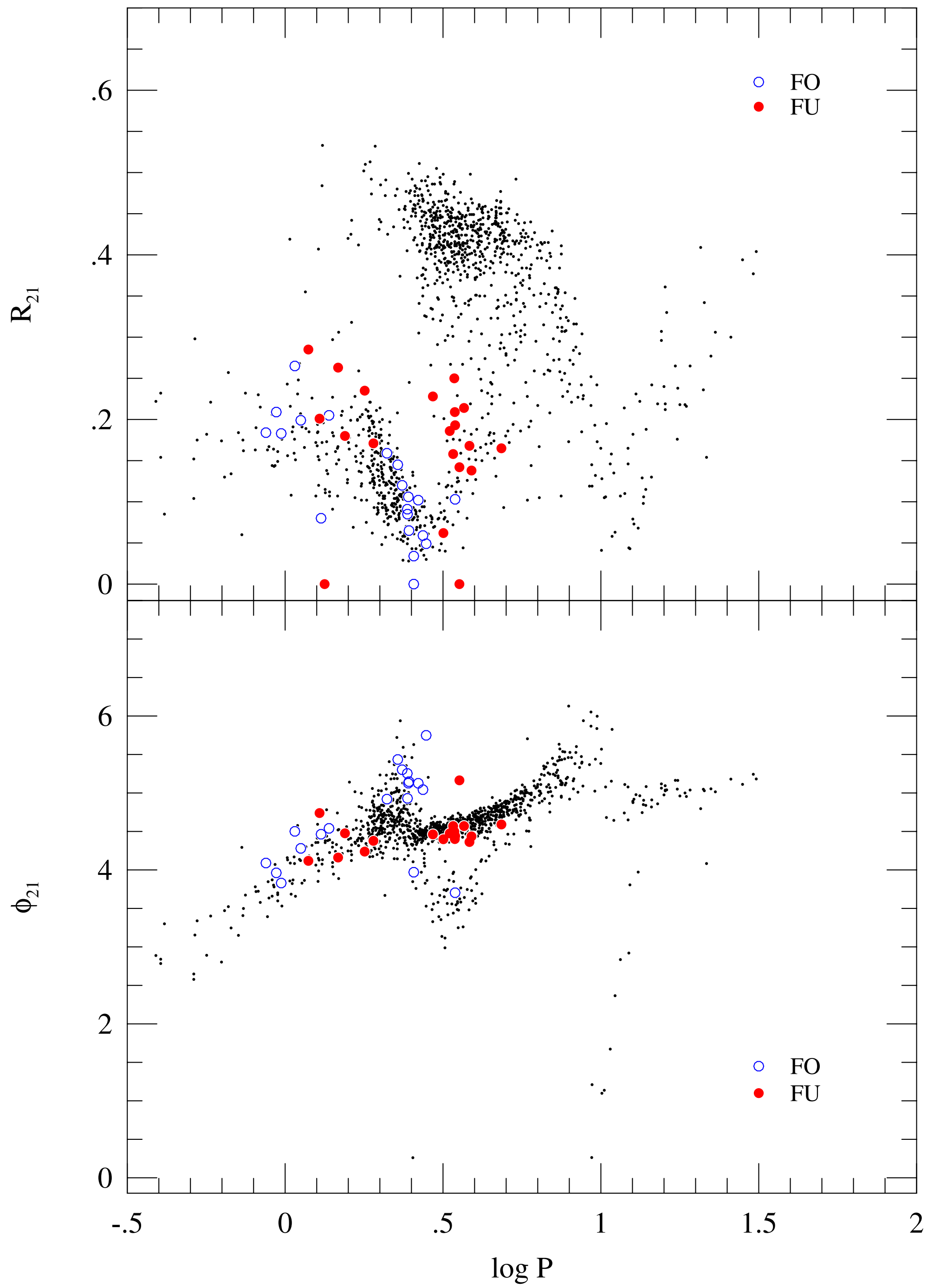

Fig. 3. R_{21} and ϕ_{21} *vs.* $\log P$ diagrams for single-mode Cepheids from the LMC (small dots). Large open and filled circles mark values of the first overtone and fundamental mode pulsations in the FU/FO double-mode Cepheids, respectively.

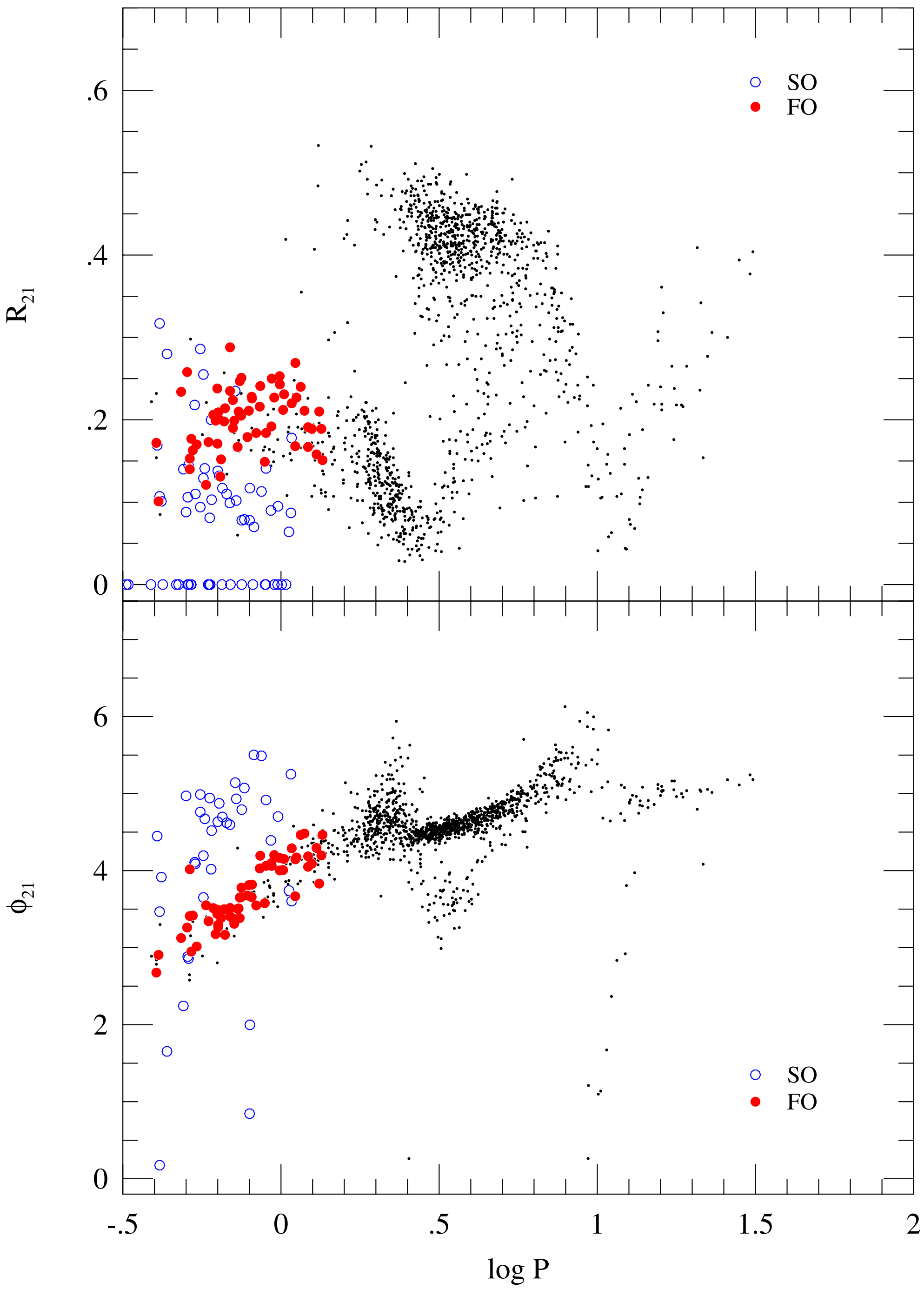

Fig. 4. R_{21} and ϕ_{21} *vs.* $\log P$ diagrams for single-mode Cepheids from the LMC (small dots). Large open and filled circles mark values of the second and first overtone pulsations in the FO/SO double-mode Cepheids, respectively.

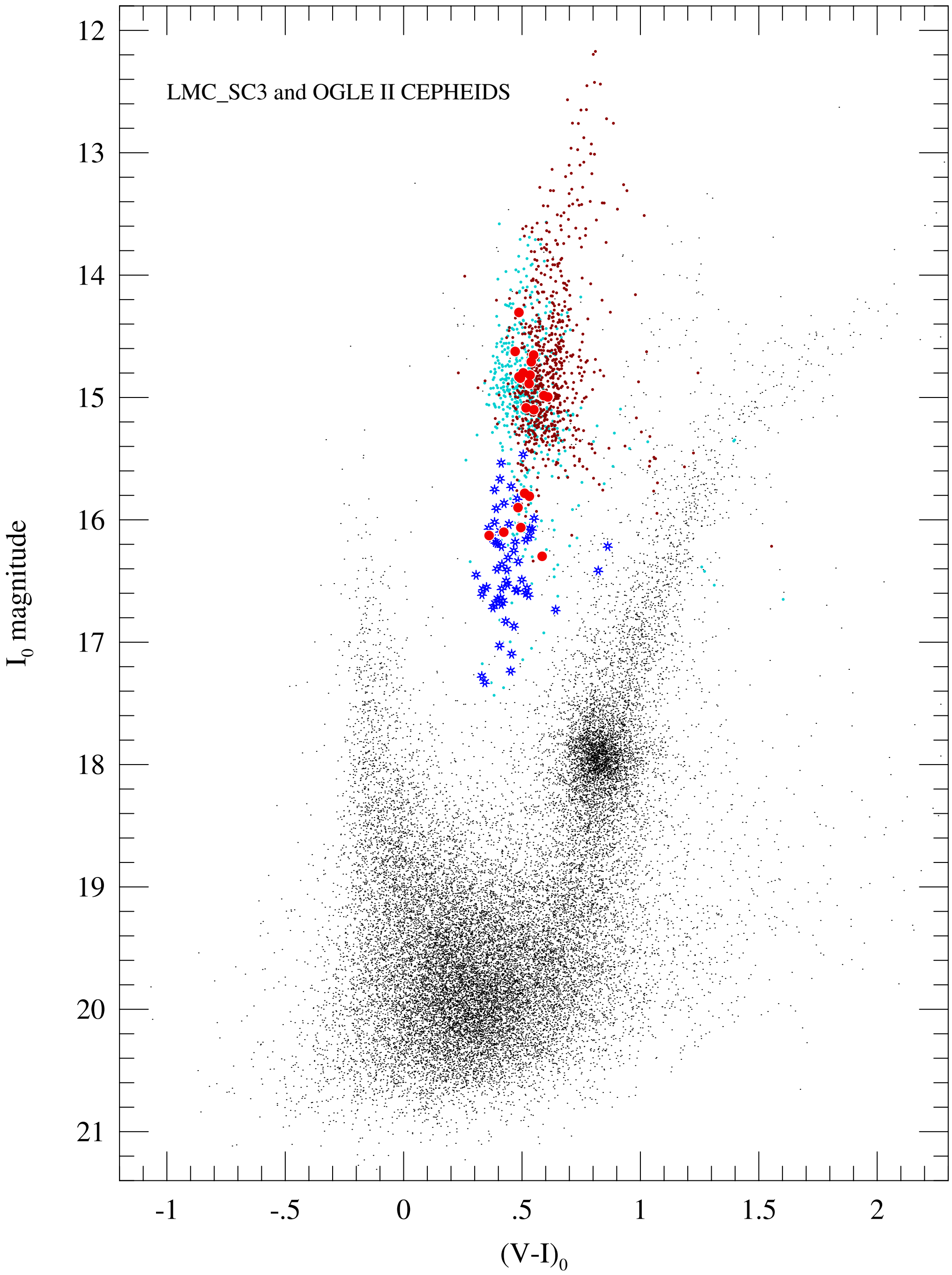

Fig. 5. Color-magnitude diagram of the LMC_SC3 field. Only about 8% of the field stars are plotted by tiny dots. Larger dots show positions of single-mode fundamental type Cepheids (darker dots) and first overtone stars (lighter dots). Large filled circles and star symbols mark positions of the FU/FO and FO/SO double-mode Cepheids, respectively.

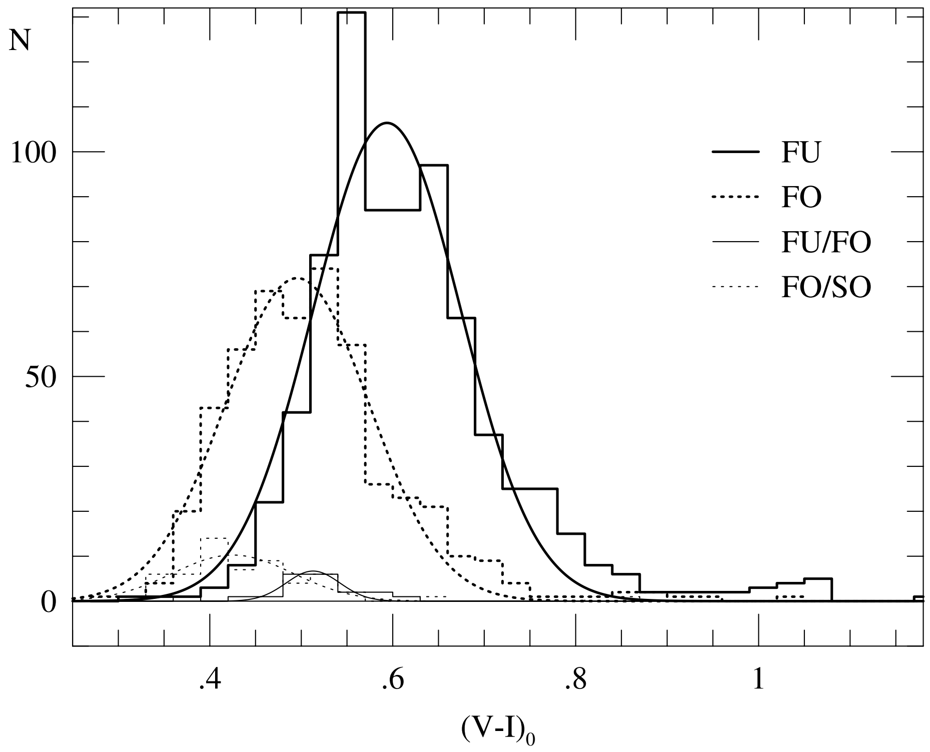

Fig. 6. Histograms of $(V-I)_0$ color distribution of single-mode and double-mode Cepheids in the LMC. Thick lines represent distribution of single-mode Cepheids: solid line – fundamental mode pulsators, dotted line – first overtone objects. Distribution of double-mode Cepheids is marked by thin line: solid line – FU/FO stars, dotted line – FO/SO Cepheids. The bins are 0.03 mag wide.

the photometry presented in Tables 1 and 2. The width of the bin is 0.03 mag. Thick solid and dotted lines correspond to the single-mode fundamental and first overtone Cepheids while thin solid and dotted lines to the FU/FO and FO/SO double-mode pulsators. All histograms were fitted with Gaussians which fit well the observed color distributions. In the case of single-mode fundamental mode Cepheids there is a small excess of red objects.

The mean $(V-I)_0$ color and the standard deviation of its distribution are: (0.425, 0.07), (0.496, 0.08), (0.513, 0.03), (0.594, 0.08) respectively for FO/SO, FO, FU/FO and FU Cepheids. Color indices (temperature) distribution depends on the type of pulsations. The single-mode first overtone Cepheids are on average by about 0.1 mag bluer than the fundamental mode pulsators. As one could expect the FU/FO double-mode Cepheids have $V-I$ color distribution in between the first and fundamental mode distributions of single-mode stars. The color distribution of FO/SO double-mode Cepheids resembles that of the single-mode first overtone stars but it is shifted bluewards.

6 Data Availability

The *BVI* photometry of the LMC double-mode Cepheids is available to the astronomical community in the electronic form from the OGLE archive:

http://www.astrouw.edu.pl/~ogle
ftp://sirius.astrouw.edu.pl/ogle/ogle2/var_stars/lmc/cep/dmcep/

or its US mirror

http://bulge.princeton.edu/~ogle
ftp://bulge.princeton.edu/ogle/ogle2//var_stars/lmc/cep/dmcep/

Acknowledgements. The paper was partly supported by the Polish KBN grant 2P03D00814 to A. Udalski and 2P03D00916 to M. Szymański. Partial support for the OGLE project was provided with the NSF grant AST-9820314 to B. Paczyński.

REFERENCES

Alcock, C. *et al.* 1995, *Astron. J.*, **109**, 1652.
Alcock, C. *et al.* 1999, *Astrophys. J.*, **511**, 185.
Pardo, I., and Poretti, E. 1997, *Astron. Astrophys.*, **324**, 121.
Roberts, D.H, Lehár, J., and Dreher, J.W. 1987, *Astron. J.*, **93**, 968.
Simon, N.R., and Lee, A.S. 1981, *Astrophys. J.*, **248**, 291.
Udalski, A., Kubiak, M., and Szymański, M. 1997, *Acta Astron.*, **47**, 319.
Udalski, A., Soszyński, I., Szymański, M., Kubiak, M., Pietrzyński, G., Woźniak, P., and Żebruń, K. 1999a, *Acta Astron.*, **49**, 1.
Udalski, A., Soszyński, I., Szymański, M., Kubiak, M., Pietrzyński, G., Woźniak, P., and Żebruń, K. 1999b, *Acta Astron.*, **49**, 45.
Udalski, A., Szymański, M., Kubiak, M., Pietrzyński, G., Soszyński, I., Woźniak, P., and Żebruń, K. 1999c, *Acta Astron.*, **49**, 201.
Udalski, A., Soszyński, I., Szymański, M., Kubiak, M., Pietrzyński, G., Woźniak, P., and Żebruń, K. 1999d, *Acta Astron.*, **49**, 223.
Udalski, A., Soszyński, I., Szymański, M., Kubiak, M., Pietrzyński, G., Woźniak, P., and Żebruń, K. 1999e, *Acta Astron.*, **49**, 437.
Udalski, A., Szymański, M., Kubiak, M., Pietrzyński, G., Soszyński, I., Woźniak, P., and Żebruń, K. 2000, *Acta Astron.*, **50**, 307.